



# Epitaxial growth of $a$ -axis oriented $\text{YBa}_2\text{Cu}_3\text{O}_{7-y}/\text{LaNiO}_3$ heterostructures on (100) $\text{SrTiO}_3$ by pulsed laser deposition

Wenbin Wu<sup>\*</sup>, K.H. Wong, P.W. Chan

*Department of Applied Physics and Materials Research Center, The Hong Kong Polytechnic University, Kowloon, Hong Kong, China*

Received 22 October 1997; revised 13 November 1997; accepted 18 December 1997

## Abstract

Conductive  $\text{LaNiO}_3$  films and  $a$ -axis oriented  $\text{YBa}_2\text{Cu}_3\text{O}_{7-y}/\text{LaNiO}_3$  heterostructures have been grown on (100)  $\text{SrTiO}_3$  substrates in situ by KrF excimer laser ablation. They were structurally characterized by X-ray diffraction in the four-circle geometry, and their transport properties were measured using of a four-probe arrangement. It was found that epitaxial  $\text{LaNiO}_3$  can be grown at temperatures from 530 to 700°C. All the as-deposited  $\text{LaNiO}_3$  films including those grown at 450°C showed good metallic transport behavior. Pure  $a$ -axis oriented  $\text{YBa}_2\text{Cu}_3\text{O}_{7-y}$  has been grown in situ on (100)  $\text{LaNiO}_3$  following a self-template deposition procedure. The epitaxial heterostructure showed an onset superconducting transition temperature of 88 K and zero resistance at 76 K. © 1998 Elsevier Science B.V.

PACS: 74.76.Bz; 81.15.Fg

Keywords: Pulsed laser deposition;  $\text{LaNiO}_3$  films;  $a$ -axis oriented YBCO/LNO heterostructures

## 1. Introduction

Recently great efforts have been devoted to the study of perovskite-related conductive oxides such as  $\text{Sr}_{1-x}\text{Ca}_x\text{RuO}_3$  and  $\text{La}_{1-x}\text{Sr}_x\text{CoO}_3$  because of their interesting transport properties, as well as their technological importance for device fabrications [1–5]. Some of these perovskites in thin film form have been used as the normal metal layer to fabricate heteroepitaxial superconductor–normal metal–superconductor (SNS) type Josephson junctions, and as

electrodes for applications in thin film ferroelectric memories [6–8]. Polycrystalline  $\text{LaNiO}_3$  (LNO) is a Pauli paramagnetic material and an n-type metallic oxide down to 0.4 K with isotropic and low resistivity (the electronic density is  $1.7 \times 10^{22} \text{ cm}^{-3}$ , and at 300 K the resistivity is about  $1 \times 10^{-5} \Omega \text{ m}$ ). It has a perovskite-related structure with rhombohedral distortion. The primitive cell of LNO consists of two formula units and it is rhombohedral with lattice parameter  $a = 5.461 \text{ Å}$  and the rhombohedral angle  $60.41^\circ$ . Pseudocubic  $a$  of this oxide is  $3.83 \text{ Å}$  [9]. Due to these electrical and structural characteristics embodied in LNO, it is believed that the thin film of LNO can act as a lattice-matched metallic oxide for heteroepitaxial SNS-type of Josephson junction with  $\text{YBa}_2\text{Cu}_3\text{O}_{7-y}$  (YBCO). In fact,  $c$ -axis oriented

<sup>\*</sup> Corresponding author. Structure Research Laboratory, University of Science and Technology of China, Academia Sinica, Hefei 230026, China. E-mail: apwbwu@hkpucc.polyu.edu.hk.

YBCO/LNO heteroepitaxial structures have been grown by several groups using pulsed laser deposition (PLD) [10,11]. In view of the longer coherence length and larger critical current density along the  $\text{CuO}_2$  plane, however,  $a$ -axis oriented YBCO over a metallic layer is more desirable for the SNS junctions. In this paper, we report on the growth and characterization of a pure  $a$ -axis oriented YBCO/LNO heterostructures. To our knowledge, this is the first report of its kind.

Although epitaxial LNO films have been laser-deposited at around  $700^\circ\text{C}$  by several groups [10–12], structural and electrical properties of the LNO films grown under different deposition conditions have not been reported. More comprehensive studies on the LNO films are therefore necessary for fabricating and understanding the YBCO/LNO heterostructures. In the following sections of this paper, the growth and characterization of LNO films prepared at different substrate temperatures and the in situ annealing of the films under various oxygen pressures will first be presented. Results on the heteroepitaxial structures will then be reported.

## 2. Growth and characterization of LNO films

The in situ growth of LNO films was carried out in a PLD system using LNO ceramic target that was prepared following the method of Wold et al. [9]. A 248 nm KrF excimer laser with 10 Hz repetition rate and  $3\text{--}4\text{ J cm}^{-2}$  energy density was used. The (100)  $\text{SrTiO}_3$  (STO) substrates of size  $10 \times 3 \times 0.5\text{ mm}$  were mounted on the heater's face plate using high-temperature silver paste. The temperature was measured by a thermocouple fixed just beneath the heater's face plate which is about 1 mm thick. An oxygen pressure of 300 mTorr was used during the growth process. The distance between the target and the substrate was kept constant at 45 mm throughout the deposition. The deposition time was 25 min for each LNO film, resulting in a final film thickness of about 250 nm. Immediately after the deposition, the LNO films were annealed in situ in 700 Torr of oxygen at the deposition temperature for half an hour. Each LNO film was structurally characterized by X-ray diffraction in the four-circle mode. Resistivity measurements of these films were performed

using a standard four-point probe method with gold contacts sputtered onto the films.

Fig. 1 shows X-ray linear scans of LNO films fabricated at substrate temperatures of  $450^\circ\text{C}$  (a),  $530^\circ\text{C}$  (b),  $610^\circ\text{C}$  (c) and  $700^\circ\text{C}$  (d). It is seen that highly-oriented LNO films with strong ( $h00$ ) reflections were prepared at deposition temperatures above  $530^\circ\text{C}$ . The X-ray  $\omega$ -scan rocking curves on the (200) reflection of the films grown at  $530^\circ\text{C}$ ,  $610^\circ\text{C}$  and  $700^\circ\text{C}$  were also recorded and the full width at half maximum (FWHM) of each film was  $1.65^\circ$ ,  $1.45^\circ$  and  $1.1^\circ$ , respectively. These values are larger than those of other epitaxial perovskite-related oxide films [1,13], and the exact reason is not clear at present. For the film deposited at  $450^\circ\text{C}$ , no reflection from the LNO was discriminated from the substrate reflections. It seems that the grown film was also highly oriented with lattice constant matched well with that of the substrate. In fact, highly oriented LNO films were

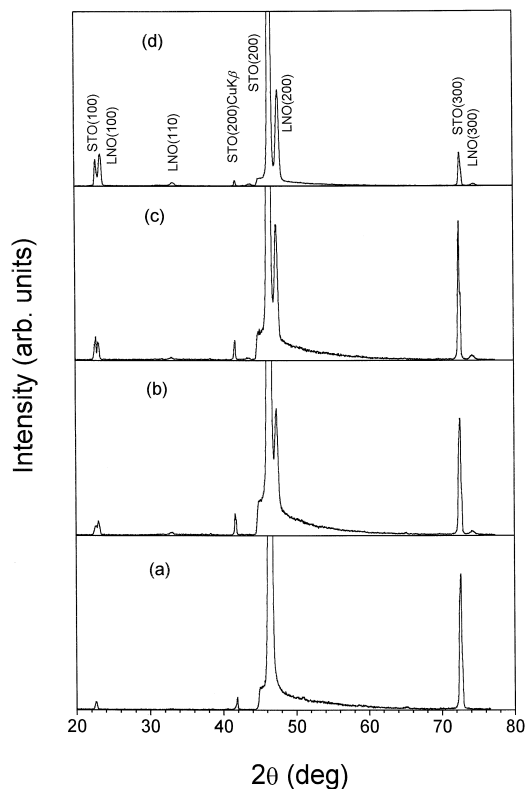


Fig. 1. X-ray diffraction  $\theta$ – $2\theta$  scans for LNO films deposited at  $450^\circ\text{C}$  (a),  $530^\circ\text{C}$  (b),  $610^\circ\text{C}$  (c) and  $700^\circ\text{C}$  (d), respectively.

prepared at substrate temperature as low as 150–250°C by Yang et al. [14] using rf magnetron sputtering on Si substrates. The lattice constant of their as-grown LNO films decreased gradually with increasing substrate temperature. A sharp decrease, however, occurred at about 500°C. PLD is generally believed to generate more energetic atomic species than other vapor deposition methods, so it is possible that the LNO film laser-deposited at the lower temperature is highly-oriented.

Fig. 2 shows the X-ray  $\phi$ -scans for the (220) reflection of the (100) STO substrate (a) and the LNO film prepared at 610°C (b). It can be seen that the film is cube-on-cube grown on the STO substrate. An epitaxial growth of the LNO films on the substrates at 530 and 700°C were also observed. Using our X-ray diffractometer, the FWHM of the peaks related to the films grown at 530, 610 and 700°C were 1.3, 1.25 and 1°, respectively, whereas the one corresponding to the (220) STO reflection was 0.5°.

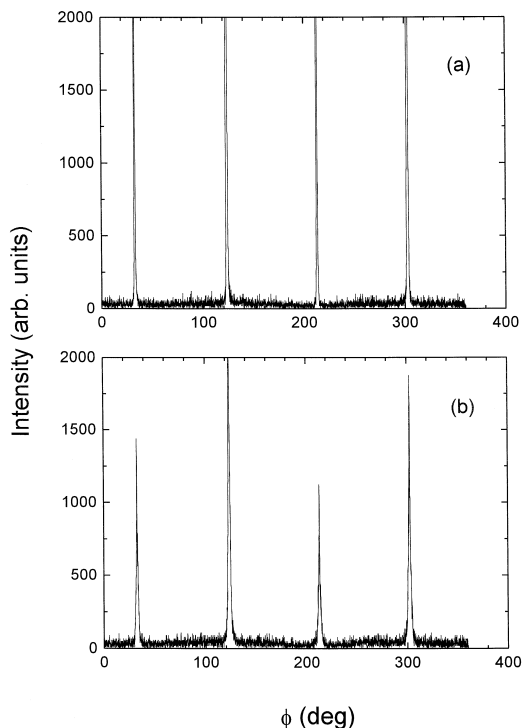


Fig. 2. X-ray  $\phi$ -scans of the (220) reflection from the (100) STO substrate (a) and the LNO film grown at 610°C (b).

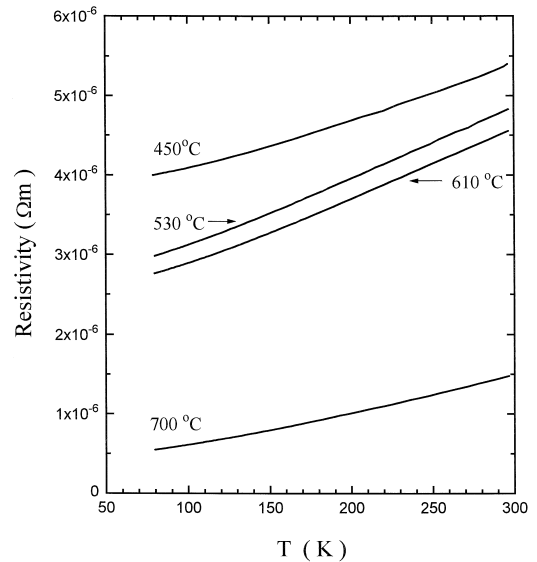


Fig. 3.  $R$ - $T$  curves of the LNO films deposited at 450–700°C as noted.

Fig. 3 gives resistance–temperature ( $R$ - $T$ ) curves of the LNO films fabricated at 450, 530, 610 and 700°C. All the films showed a metallic transport behavior, and with deposition temperature increased from 450 to 700°C, resistivity at room temperature of the as-grown films decreased from around  $5.5 \times 10^{-6}$  to  $1.5 \times 10^{-6} \Omega \text{ m}$ , which is consistent with results reported by other groups [12,14]. Moreover, the good metallic transport behavior of these LNO films was less sensitive to the in situ annealing oxygen pressure than other perovskites such as  $\text{La}_{0.5}\text{Sr}_{0.5}\text{CoO}_3$  films. For example, the as-grown LNO films annealed in situ at  $\sim 10^{-3}$  Torr  $\text{O}_2$  atmosphere was also metallic (not shown). For  $\text{La}_{0.5}\text{Sr}_{0.5}\text{CoO}_3$  conductive films, however, it usually showed a semiconducting transport behavior when annealed at reducing  $\text{O}_2$  pressure [4,13]. This property of LNO may be important to the superconducting properties of epitaxial YBCO/LNO heterostructures.

### 3. Growth and characterization of YBCO/LNO heterostructures

The growth of YBCO/LNO heterostructures was conducted using the same PLD setup. In order to

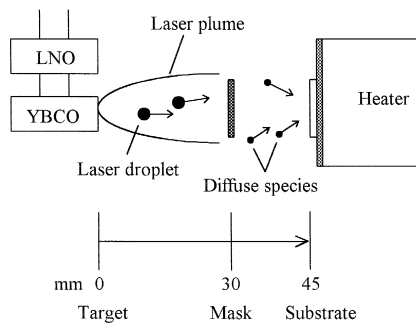


Fig. 4. Schematic of arrangement of target, mask, substrate and laser plume.

eliminate the laser droplets from the ceramic YBCO target, a shadow mask of 10 mm  $\times$  10 mm was introduced into the vacuum chamber and placed between the target and substrate. The target–substrate distance and the substrate–mask distance were 45 and 15 mm, respectively. This ‘eclipse method’ proposed by Kinoshita et al. [15] has proved to be very effective to eliminate the laser droplets that are detrimental for fabricating thin film devices. Very recently, Trajanovic et al. [16] quantitatively demonstrated that this method can help to improve film surface smoothness, thickness uniformity, as well as to maintain stoichiometric composition from target to film. A schematic of the target, mask and substrate arrangement was shown in Fig. 4. Both the LNO and YBCO films were deposited in the same vacuum run. During deposition, oxygen pressure of 400 mTorr was employed. After the LNO film deposition (with or without the shadow mask, no different structural and electrical properties of the as-grown LNO films were observed), the YBCO film was grown following a self-template deposition procedure [17]. Briefly, the film was first grown at 640°C for 5 min and then, without stopping the deposition, the substrate temperature was increased to 750°C at 15°C/min, and the YBCO target was further ablated for 25 min. After deposition, the YBCO/LNO bilayer was in situ annealed at 700 Torr of oxygen at 500°C for 30 min and then cooled down slowly to room temperature.

Fig. 5 is an X-ray linear scan from the YBCO/LNO bilayer with the LNO layer grown at 700°C for 10 min. It is clear that only the ( $h00$ ) LNO and ( $h00$ ) YBCO reflections were recorded,

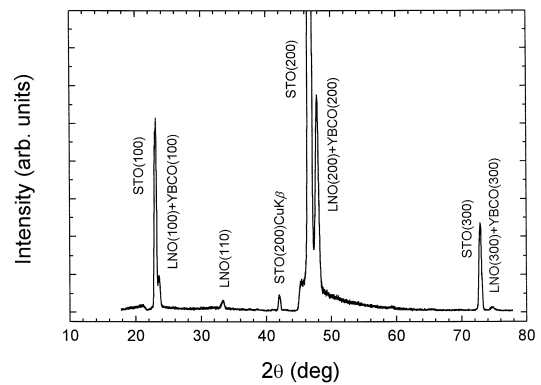


Fig. 5. An X-ray linear scan of the  $a$ -axis oriented YBCO/LNO bilayer deposited on (100)STO substrate.

and the reflections with the same order were overlapped. Fig. 6a,b shows the X-ray  $\phi$ -scan curves on the (102) YBCO reflection of the YBCO/LNO bilayers with the LNO film deposited at 550 and 700°C. They suggest that a cube-on-cube growth of

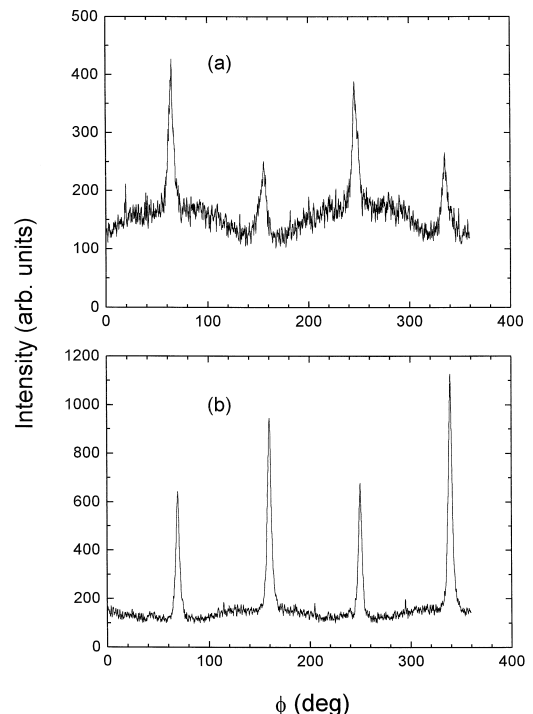


Fig. 6. X-ray  $\phi$ -scans of the (102) YBCO reflection from  $a$ -axis oriented YBCO/LNO heterostructures with the LNO layer deposited at 550 (a) and 700°C (b).

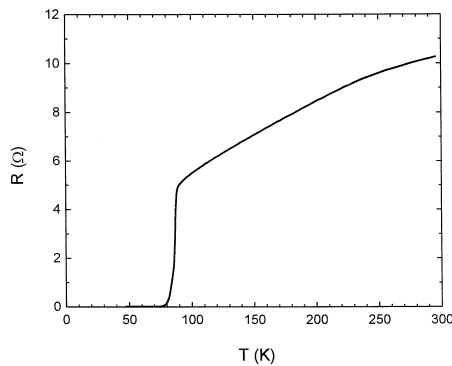


Fig. 7.  $R$ - $T$  curve of the  $a$ -axis oriented YBCO/LNO bilayer with the LNO layer grown at 700°C.

the  $a$ -axis oriented YBCO has been obtained on the epitaxial LNO films, and when the LNO film deposited at higher temperature was used, the crystallinity of the epitaxial and  $a$ -axis oriented YBCO layer improved dramatically. For the  $a$ -axis oriented YBCO/LNO heterostructure with the LNO grown at lower temperature, a drop of resistance at about 80 K was observed, but no zero resistance was recorded until 30 K. Fig. 7 shows a  $R$ - $T$  curve of the YBCO/LNO bilayer with the LNO grown at 700°C. The superconducting transition set on at 88 K and ended at 76 K.

Contacts between YBCO and metallic perovskite-type oxide films are important for both the fabrication of vertical-type SNS junctions and the metallization of high- $T_c$  superconductor thin films and devices. High-quality  $c$ -axis oriented YBCO films with  $T_c$  ( $R = 0$ ) near 90 K have been grown on SrRuO<sub>3</sub> and LNO films [3,10]. Few results, however, have been reported on the growth of  $a$ -axis oriented YBCO on metallic oxide films. Although further optimization is surely needed, our results have demonstrated that  $a$ -axis oriented superconductive YBCO over a metallic oxide is feasible. The superconductivity of  $a$ -axis oriented YBCO films is usually affected by structural defects such as the oxygen disorder. According to our results, however, properties such as the crystallinity of the underlying metallic oxide layer may also be another factor needed to be considered. As mentioned before, the 'eclipse method' of PLD has proved to be effective to eliminate the laser droplets, and it was shown that with this method, high-quality  $c$ -axis oriented YBCO films can be

produced [15]. The present results also demonstrated that superconductive  $a$ -axis oriented YBCO films can be grown by use of this method.

#### 4. Summary

Epitaxial LNO films have been grown at substrate temperature ranging from 530 to 700°C. Highly-oriented LNO film could be prepared by PLD at lower temperatures. All as-grown LNO films showed a good metallic transport property, and it is less sensitive to oxygen annealing pressure than other conductive perovskites such as La<sub>0.5</sub>Sr<sub>0.5</sub>CoO<sub>3</sub>. It has been demonstrated that by using the 'eclipse method' of PLD, superconductive  $a$ -axis oriented YBCO films can be grown on LNO metallic films, and the resulting heterostructure showed a  $T_c$  onset at 88 K and zero resistance at 76 K.

#### Acknowledgements

This work was partially supported by the Hong Kong Research Grant Council under code number HKP 152/93E.

#### References

- [1] C.B. Eom, R.J. Cava, R.M. Fleming, J.M. Phillips, R.B. van Dover, J.H. Marshall, J.W.P. Hsu, J.J. Krajewski, W.F. Peck Jr., *Science* 258 (1992) 1766.
- [2] L. Klein, J.S. Dodge, C.H. Ahn, G.J. Snyder, T.H. Geballe, M.R. Beasley, A. Kapitulnik, *Phys. Rev. Lett.* 77 (1996) 2774.
- [3] X.D. Wu, S.R. Foltyn, R.C. Dye, Y. Coulter, R.E. Muenchausen, *Appl. Phys. Lett.* 62 (1993) 2434.
- [4] J.T. Cheung, P.E.D. Morgan, D.H. Lowndes, X.-Y. Zheng, J. Breen, *Appl. Phys. Lett.* 62 (1993) 2045.
- [5] A. Chainani, M. Mathew, D.D. Sarma, *Phys. Rev. B* 46 (1992) 9976.
- [6] K. Char, L. Antognazza, T.H. Geballe, *Appl. Phys. Lett.* 63 (1993) 2420.
- [7] R. Ramesh, H. Gilchrist, T. Sands, V.G. Keramidas, R. Haakenaasen, D.K. Fork, *Appl. Phys. Lett.* 63 (1993) 3592.
- [8] C.B. Eom, R.B. Van Dover, J.M. Phillips, D.J. Werder, J.H. Marshall, C.H. Chen, R.J. Cava, R.M. Fleming, D.K. Fork, *Appl. Phys. Lett.* 63 (1993) 2570.
- [9] A. Word, B. Post, E. Banks, *J. Am. Chem. Soc.* 70 (1957) 4911.

- [10] K.M. Satyalakshmi, R.M. Mallya, K.V. Ramanathan, X.D. Wu, B. Brainard, D.C. Gautier, N.Y. Vasanthacharya, M.S. Hegde, *Appl. Phys. Lett.* 62 (1993) 1233.
- [11] D. Kumar, R.D. Vispute, O. Aboelfotoh, S. Oktyabrsky, K. Jagannadham, J. Narayan, P.R. Apte, R. Pinto, *J. Electron. Mater.* 25 (1996) 1760.
- [12] T. Yu, Y.-F. Chen, Z.-G. Liu, X.-Y. Chen, L. Sun, N.-B. Ming, L.-J. Shi, *Mater. Lett.* 26 (1996) 73.
- [13] P.W. Chan, W. Wu, K.H. Wong, K.Y. Tong, J.T. Cheung, *J. Phys. D* 30 (1997) 957.
- [14] C.-C. Yang, M.-S. Chen, T.-J. Hong, C.-M. Wu, J.-M. Wu, T.-B. Wu, *Appl. Phys. Lett.* 66 (1995) 2643.
- [15] K. Kinoshita, H. Ishibashi, T. Kobayashi, *Jpn. J. Appl. Phys.* 33 (1994) L417.
- [16] Z. Trajanovic, S. Choopun, R.P. Sharma, T. Venkatesen, *Appl. Phys. Lett.* 70 (1997) 3461.
- [17] M. Mukaida, S. Miyazawa, *Appl. Phys. Lett.* 63 (1993) 999.